Performance Evaluation of a Modified DC Compressor Powered by Solar Energy

Orhan Ekren*

Ege University, Solar Energy Institute, Bornova, Izmir 35100, Turkey

Abstract: In this study, a modified direct current compressor (MDC) is tested experimentally. The experimental study is conducted in order to observe the performance of a solar energy powered MDC. Then, the performance of this MDC is compared with brand new direct current compressors (BNDC) in the market. The experimental setup has a mini fridge with 50 liters capacity, a photovoltaic panel, a battery, a charge regulator and measurement equipments. Also, a pyranometer is used to define solar radiation on the photovoltaic panel. Experiments are conducted for various cabinet loads such as no storage items, low, nominal and over load at steady state condition.

Keywords: Photovoltaic, solar energy, DC compressor, energy analysis, mini fridge, solar radiation.

1.INTRODUCTION

Since HVAC&R systems are one of the most common used equipments and the high energy consumed equipments, decreasing energy usage and improving efficiency is important in these systems. This may help to decrease the expenses as well as to create environmental friendly systems in the worldwide. Mostly, energy savings in refrigeration systems are realized *via* optimum working conditions by using control techniques. Although these methods provide savings, they may not provide environmental friendly solution. Therefore, environmental friendly systems should be developed.

Direct current (DC) compressor usage instead of alternative current (AC) provides opportunity using renewable energy sources also may help energy savings in refrigeration systems. Since DC applications require low voltage and direct current supply such as 12-24 volts. Small refrigerator usage is very common at many vehicles and domestic requirements. Using a DC compressor in a small refrigeration system provides a big opportunity to supply the energy by renewable energy technologies such as solar or hybrid of renewable sources because of their low power requirement. Since small refrigerator usage is very common, decreasing energy usage and improving efficiency on these systems may have big potential of savings. Some investigations have been conducted concerned with the renewable energy assisted refrigeration systems in the literature. These studies can be classified as analysis of AC compressor powered by solar energy *via* inverter and analysis of DC compressor powered by solar energy. Ewert *et al*. [1] studied refrigeration systems supplied by batteries and solar energy. They investigated three different cooling technologies such as free piston stirling, thermoelectric and vapor compression with DC compressor in the same vacuum insulated cabinet which is 365 liters. Also phase change material is used in the cabinet for thermal energy storage. In the experimental study, coefficient of performance (COP) of three systems is compared at steady state conditions. Results showed that COP is 0.04, 0.14 and around 1 for the thermoelectric solar refrigerator, stirling cooler and vapor compression cycle, respectively. Kattakayam and Srinivasan [2] is investigated AC operated domestic refrigerator powered by solar energy with a battery bank and an inverter for vaccine storage. This paper presents cool-down, warm-up and steady state performance of domestic refrigerator which has an internal volume of 165 liters, 100 W cooling capacity and uses CFC-12 refrigerant. According to the results of conducted experiments this kind of refrigerators could be used to improve the energy efficiency of domestic refrigerators. Also, performance can be improved by switching cabinet with vacuum insulated panels since heat leak contributes maximum to the cooling capacity. However, vaccine storage near wall of the door should be avoided. Cherif and Dhouib[3] presented performances, simulation responses and dynamic behavior of a solar energy powered refrigeration plant using latent storage at several climatic conditions and under load disturbances. They used a new storage strategy which allows to evaluate solar energy system reliability and to compare its performance with classic battery storage system. According to them, efficiency of the system and its performance decrease relatively with solar radiation disturbance because solar energy system requires good climatic conditions to reach the

*Address correspondence to this author at the Ege University Solar Energy Institute 35100 Bornova, Izmir, Turkey; Tel: +90 232 311 5011;
E-mail:orhanekren@gmail.com

E-ISSN: 2409-5826/17

storage regime. Kaplanis and Papanastasiou [4] described design and development stages to convert a conventional refrigerator to a solar powered one. Changes on a conventional refrigerator are introduced to reduce cooling load and required power. Tests are conducted to define performance of the refrigerator components especially compressor as well as the refrigerator as a whole. Kim and Ferreira [5] presented a review study for different refrigeration technologies used by solar energy. The technologies given in the review are solar electric such as vapor compression cycle with DC compressor, stirling refrigeration and magnetic refrigeration. Solar thermal systems cover thermo-mechanical, absorption, adsorption and desiccant solutions. A comparison is made between different solutions with respect to energy efficiency and economic feasibility. According to this comparison solar electric and thermo-mechanical systems are more expensive than thermal sorption systems. Modi *et al*. [6] studied converting procedure of a 165 liters domestic refrigerator with AC compressor to solar powered one. They used a household refrigerator for this purpose and re-designed by adding a battery bank, an inverter and a transformer. New refrigerator is supplied by solar energy. They conducted some performance tests to define performance of the system and concluded that COP decreases with time from morning to afternoon and a maximum COP is 2.102. This COP value is obtained at 7 AM. They also studied economic feasibility of the system at the climatic conditions in Jaipur-India. According to their analysis the new solar energy powered refrigerator with AC compressor is economic with carbon trading option.

In this study, performance analysis of a MDC is experimentally tested in terms of cooling capacity, power consumptions, *COP, COP*$_{Car}$, percentage of *COP*$_{Car}$ and effectiveness of the evaporator. The contribution of this study is comparison of the MDC with BNDC. Also define applicability of the modification procedure.

2. DESCRIPTION OF THE EXPERIMENTAL SETUP

In the experimental setup, a mini fridge with DC hermetic compressor and capillary tube as an expansion device are used. The fridge's internal volume is 50 liters and its evaporator is roll-bond type. The condenser is an embedded copper pipe in the fridge body. R134a is used as a refrigerant. DC compressor is powered by a photovoltaic panel (PV) with 80 W capacity and 0.65 m^2 surface area. In the experimental setup, also a battery with 80 Ah capacities and a charge regulator are used. Several temperatures are monitored in the cooling cycle in order to realize a proper performance analysis. These locations are the suction and the discharge of the DC compressor, inlet and outlet of the condenser and the evaporator. Also, temperatures are measured on the

Table 1: Specifications of the Measuring Equipments

Equipments	Specifications	
Pressure Transducer	Type : Carel SPKT, Ratio–metric	
	Range : Low pressure *(Between -1 and 9 bar)*,	
		High pressure *(Between 0 and 45 bar)* absolute
	Output Signal : 0-5 VDC	
	Accuracy : ±1.2% of full scale at 25°C	
Thermocouples	Type	: T
	Range : -200 and 350 °C	
	Output Signal : mVDC	
	Accuracy : ±0.4 % of full scale	
Wattmeter	Type	: BS157
	Range : 220/600 V , 50/60 Hz	
	Accuracy : ±%1.5	
Pyranometer	Type	: Epply 8-48 Black&White (ISO 2nd Class)
	Range :0 – 1500 W m^{-2}	
	Output : 15μV (W m^{-2})$^{-1}$	
	Accuracy : 0.5 % in the range 0.5 and 1330 W m^{-2}	

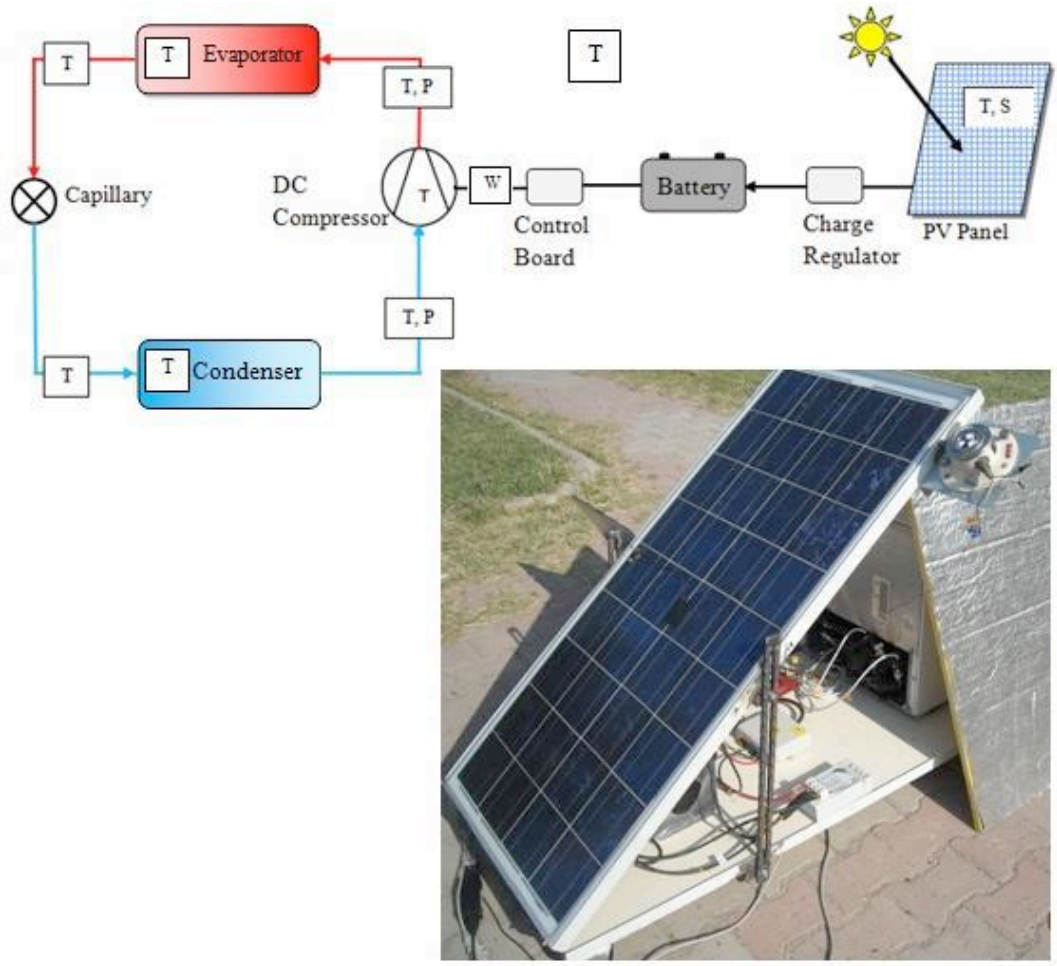

Figure 1: Solar energy powered fridge setup.

fridge freezer surface being used as an evaporator, on the fridge outside surface being used as a condenser, in the cabinet, on the DC compressor surface, on the PV surface and ambient with 5 seconds interval. Insulated copper-constantan (type T) thermocouples are used for temperature measurements.

In addition to temperatures, pressures are measured at the suction and the discharge line of the compressor by ratio-metric type pressure transducers. To be able to complete a reasonable energy analysis, solar radiation on the 45^{o} tilted PV surface is measured by a pyranometer. Measuring equipment specifications are given in Table **1**.

Experimental setup is illustrated in Figure **1**. In this figure, letters *T*, *P*, *W* and *S* show temperature, pressure, power input and solar radiation measurement points, respectively.

DC compressor supply voltage may be 12-24 VDC and current may be higher than AC compressor's which has same power input because of low supply voltage. Higher current input may require a battery between compressor and PV to provide required torque to the compressor. In the current study, the compressor is powered by a lead acid type battery with 85% discharge efficiency for eight hours at no sun period. The DC compressor used in this study is not an original brand new one. It is converted from a reciprocating type hermetic AC compressor by modifying electrical motor stator wiring. Therefore it is named as 'modified DC' in the paper. To able to change the stator wiring, AC compressor's dome is opened and after a new wire arrangement, it is welded back. The main aim of this study is to analyze whether the MDC's cooling capacity is close enough to a BNDC's cooling capacity in the market or not. Comparisons are conducted with a BNDCs' catalogue values. They are ACC GD30FDC and Danfoss BD35F [7, 8].

2.1. Compressor Modification Procedure

Compressors are composed of a mechanical compression part and an electrical motor. Basically, an

Table 2: Specifications of DC Compressors

	Modified DC Compressor	Original DC Compressor (ACC GD30FDC)	Original DC Compressor (Danfoss BD35F)
Displacement (cm^3)	2.00	3.00	2.00
Speed (rpm)	2000	2000	2000
Compressor Capacity ($m^3\ s^{-1}$)	$6.7x10^{-5}$	$7.5x10^{-5}$	$6.7x10^{-5}$
Motor Type (-)	Brush-less	Brush-less	Brush-less
Current (Amp)	4.13	2.83	2.80
Voltage (VDC)	12	12	12
Winding Resistance (Ohm)	0.98	0.80	2.20
Phase Number (-)	3	3	3
Pole Number (-)	6	6	6
Start Type (-)	Electronic	Electronic	Electronic

electric motor converts electrical energy to mechanical energy in a refrigeration compressor. Refrigerant is being compressed from low pressure to high pressure by this mechanical energy at the compression part. Size of the compression part defines the capacity of the compressor. Capacity of the compressor is significant in a refrigeration system because cooling effect of a refrigeration system mainly depends on it. Capacity of the reciprocating compressor is total amount of displacement per unit time. Displacement of a piston equals to volume swept by the piston inside the cylinder. A reciprocating compressor's displacement defines by diameter of cylinder bore, length of piston stroke inside the cylinder, number of cylinders in the compressor and rotation speed of crankshaft. In general, the capacity formula is;

$$C = nc * (\pi * d^2 * L) * N \quad (1)$$

where *nc* is number of cylinder in the compressor, *d* is radius of cylinder bore, *L* is stroke of piston and *N* is rotation speed of crankshaft or rotational speed of the motor. The compressor used in the study is reciprocating type and its displacement is 2.0 cm^3. Compression part is remained same after modification of the AC compressor to the DC one. Compression unit specifications are shown in Table **2**.

AC to DC modification is realized on electrical motor. The electrical motor of the compressor is an AC induction type and after modification it is used as a brushless DC motor. Electrical motor specifications are shown in Table **2**. Both AC induction and brushless DC motors are the most common motors for refrigeration compressors [9]. An electrical motor is composed of a rotor, a stator and windings [10, 11, 12]. Rotor is rotating and stator is stationary in the motor. Stator is composed of many thin metal sheets and has slots.

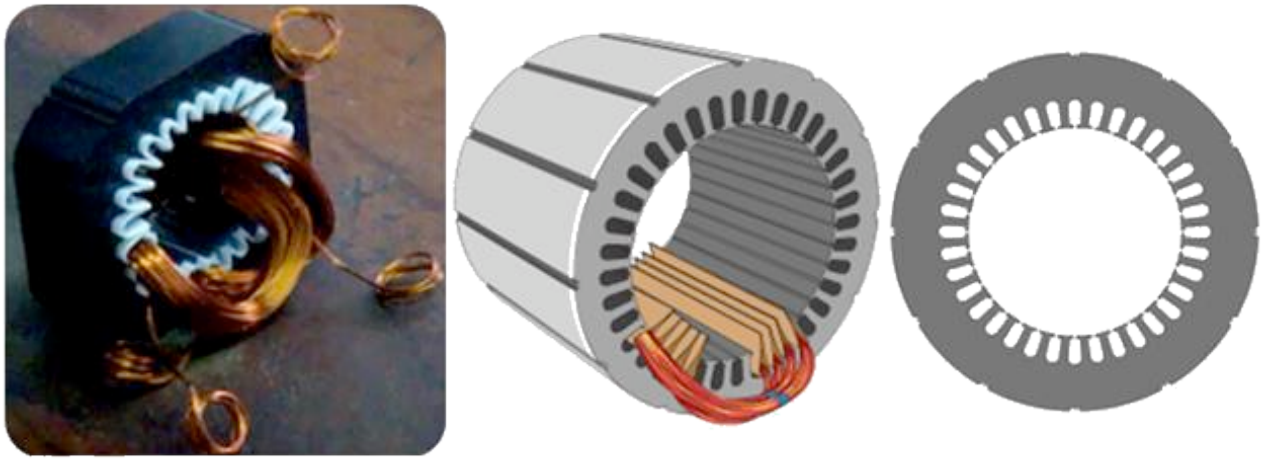

Figure 2: Stator slots and winding [10].

Coils of winding are inserted into slots of the stator as shown in Figure **2**. When an assembled motor is in operation, the stator windings are connected directly to the power source.

There is a relation between stator voltage, magnetic flux and radian speed [11,12],

$$V = K * \Phi * w \quad (2)$$

K is motor constant, ϕ is magnetic flux and *w* is radian speed. The relation between radian speed and rotational speed of the motor (*N*) is [11, 12].

$$w = \frac{2*\pi*N}{60} \quad (3)$$

DC motor output power (*Pm*) is directly proportional to stator voltage (*V*) and current (*I*). Developed torque of a brushless DC motor can be defined as [11, 12]

$$T_d = \frac{P_m}{w} = \frac{V*I}{w} = K * \Phi * I = \frac{9.55*P_m}{N} \quad (4)$$

For an electrical motor, number of stator slots (24 slot in the current stator) and winding pattern are key design parameters since the total number of turns of coil per phase is directly proportional to the torque of DC motor [11, 12, 13]. Total number of turns of coil also effects the amount of magnetic field [11, 12, 13]. Magnetic field can be calculated with magnetic flux, stator length (*l*), and stator radius (*r*) [11];

$$B = \frac{\Phi}{l*r} \quad (5)$$

Resistance of a coil in ohm can be calculated by [12];

$$R = \frac{\rho*Lm*}{A} * n \quad (6)$$

where ρ is resistivity of conductor in mm m^{-2} (copper is used in the current stator), *Lm* is mean length of each turns in m and *A* is area of cross-section of the conductor in mm^2 and *n* is the number of turns.

In the current study, power of the AC compressor is same with the MDC's power which is desired as 1/15 hp. Input voltage of the modified brushless DC motor is 12 VDC and rotational speed is 2000 rpm. Stator length and radius of the DC motor are 6 cm and 5 cm, respectively. According to the brushless DC motor design procedure, the copper wire diameter is calculated as 0.3 mm, the total wire length for per phase is calculated as 5 m and the number of turns of coils in the stator is calculated as 34. After these calculations, the modification is realized by the replacement of stator windings in the compressor. Figure **3** shows the modified compressor. This modification procedure can be applied for AC compressors having electrical motor failure which have not completed their life cycles yet.

Figure 3: Modified DC compressor.

3. EXPERIMENTAL STUDY AND RESULTS

Experiments are carried out while for four cabinet fullness condition: no storage, low, nominal and over load. In the low, nominal and over load conditions, it is considered that there are 5, 10 and 15 liters water in the cabinet, respectively. The compressor is analyzed at the steady state conditions. The performance of the system is analyzed in terms of cooling capacity, *COP*, *COPCar*, percentage of *COPCar* and effectiveness of the evaporator. Cooling capacity is calculated by;

$$q_{cooling} = UA(T_{amb} - T_{cab}) \quad (7)$$

where *UA* is total heat transfer coefficient of the mini fridge cabinet which is obtained by reverse heating method as 0.5 W $^{o}C^{-1}$ *Tamb* and *Tcab* are ambient and cabinet temperatures, repectively. Coefficient of performance of the compressors is;

$$COP = \frac{q_{cooling}}{W_{com}} \quad (8)$$

where *Wcom* is compressor power input. This value is measured by a wattmeter. *COPCar* and percentage of *COPCar* are calculated by equations (8) and (9), respectively.

$$COP_{Car} = \frac{Tevap}{Tcond - Tevap} \quad (9)$$

where *Tcond* and *Tevap* are condensing and evaporating temperatures, respectively. Percentage of *COPCar* shows the potential that has already been used;

$$\%COP_{Car} = \frac{COP}{COP_{Car}} * 100 \quad (10)$$

Effectiveness value of the evaporator is;

$$\varepsilon_{HX} = \frac{q}{qmax} = \frac{T_{C_o} - T_{C_i}}{T_{H_i} - T_{H_o}} \quad (11)$$

where *q* and *qmax* can be calculated as;

$$q = C_H * \left(T_{H_i} - T_{H_o}\right) = C_C * \left(T_{C_o} - T_{C_i}\right) \quad (12)$$

$$q_{max} = C_{min} * \Delta T_{max} = C_{min} * \left(T_{H_i} - T_{C_i}\right) \quad (13)$$

where *TC* and *TH* are cold and hot side fluid temperatures respectively. Substitutes, o is outlet and i is inlet of fluid. Hot side and cold side fluid specific heats are *CH* and *CC*, respectively. In the present study, fluid in the cold side is refrigerant R134a flowing inside the evaporator and fluid in the hot side is the air which is already in the cabinet. Specific heat of the R134a is

Table 3: Experimental Results for Modified DC Compressor

	Unit	No Items	Low Load	Nominal Load	Over Load
Psuc	bar	0.671	0.600	0.500	0.400
Pdisc	bar	11.318	11.400	11.600	12.000
Tcom_o	°C	77.661	78.661	82.323	86.312
Tcon_o	°C	38.697	43.186	43.631	44.855
Tcpl_i	°C	37.360	35.600	38.300	38.862
Tevp_i	°C	-14.257	-3.728	-1.639	-1.108
Tevp_o	°C	-8.226	3.728	4.639	5.108
Tcom_i	°C	42.081	46.542	46.949	48.646
Tcond	°C	44.096	47.723	48.090	50.096
Tevap	°C	-17.257	-6.728	-4.639	2.108
Tamb	°C	30.431	30.971	30.872	30.396
Tcab	°C	-4.560	11.893	14.137	18.999
Tcom_srf	°C	51.441	61.293	63.586	65.708
Tpv_srf	°C	44.864	44.666	46.218	45.372
Sinst_tilt	Wm^{-2}	937.670	937.670	937.670	937.670
Current	Amp	4.133	4.144	4.320	4.433
Input Power	W	49.199	50.063	52.156	53.199
Cooling Capacity	W	17.496	9.539	8.367	5.699
COP	-	0.356	0.191	0.160	0.107
COPCar	-	4.177	4.899	5.099	5.743
%COPCar	-	8.514	3.889	3.146	1.865
εHX	-	0.622	0.477	0.398	0.309
m	$kg\ s^{-1}$	0.00243	0.00296	0.00257	0.00236
ηcomp	-	0.2264	0.1782	0.1978	0.1994

lower than the air. Therefore, minimum specific heat (C_{min}) is equal to the specific heat (C_{R134a}) of the cold side fluid. Experimental results for different cooling load are given in Table **3**. Steady-state conditions are obtained 3 hours later. Experiments are carried out at the lowest temperature set of the cabinet for the all loads.

To define the performance of the MDC, measured and calculated values are analyzed. It is observed that when the cabinet loads increases, discharge temperature and pressure of the compressor also increase because of high amount of evaporation (superheating). It is also noted that at the higher level of superheat, the refrigerant specific volume increases. This results with lower refrigerant compression at the same power input. Therefore, cooling capacity and *COP* decrease at high levels of superheat. Besides, it is observed that isentropic efficiency of the MDC decreases with the increased superheating.

In this section, only the results of experiments when there is no storage item in the cabinet are given in graphic formats. The cabinet temperatures are illustrated in Figure **4**. According to that the lowest temperature that the cabinet reached is about -4.5°C for the present solar powered DC refrigeration system.

Evaporating and condensing temperatures are shown in Figure **5**. These temperatures give information about Carnot efficiency and also conditions in the evaporator and condenser.

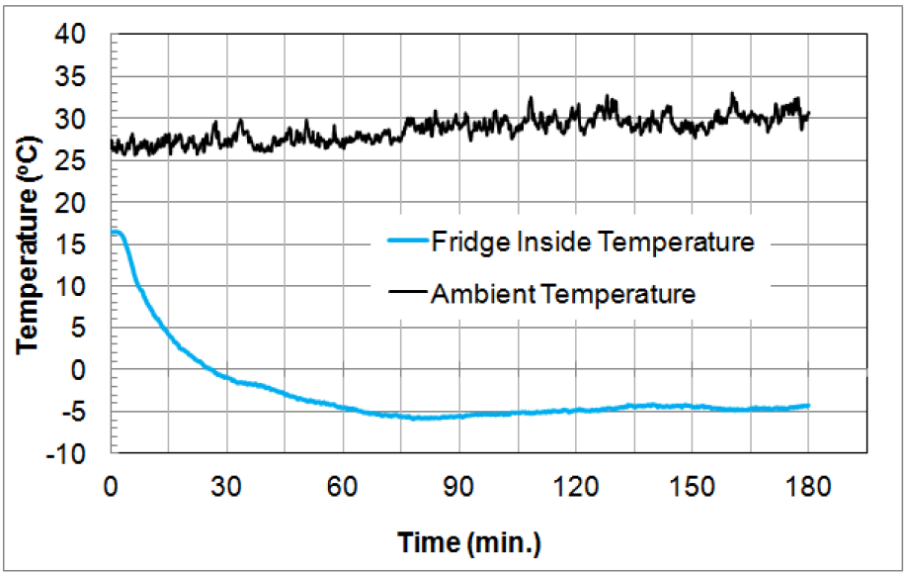

Figure 4: Fridge inside and environment temperatures.

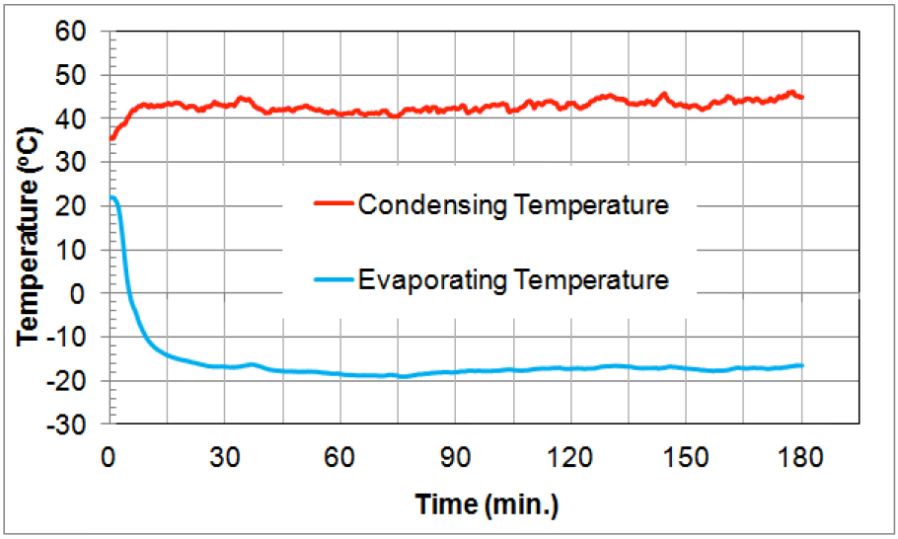

Figure 5: Evaporating and condensing temperatures.

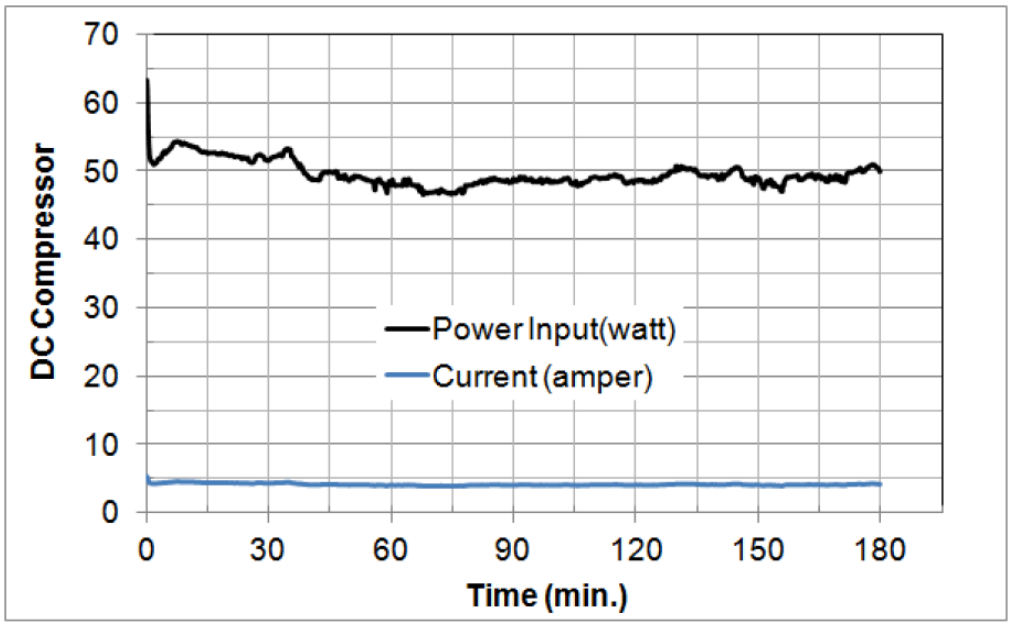

Figure 6: Compressor current and power input.

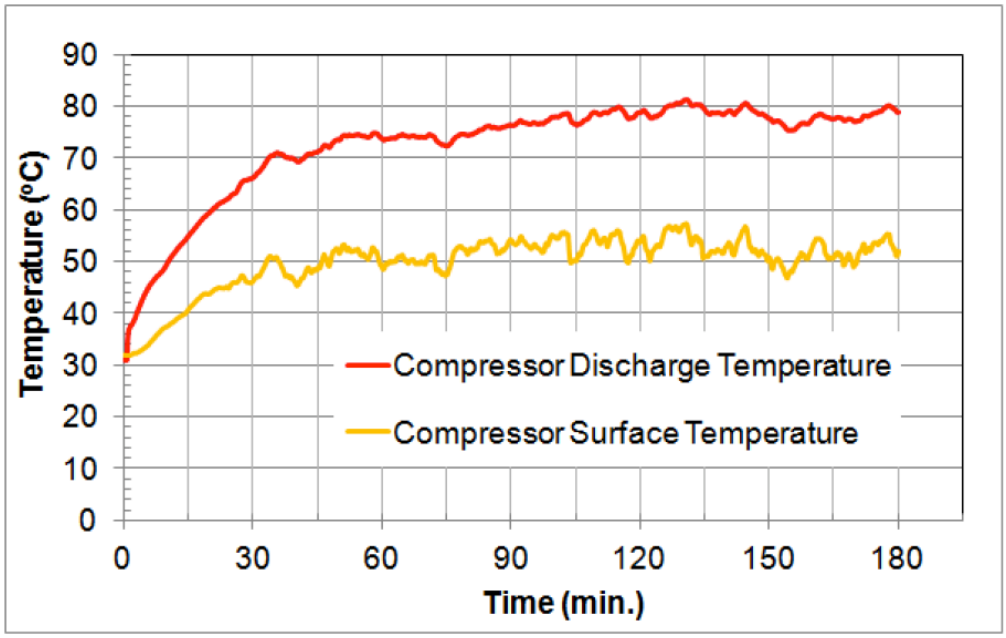

Figure 7: Compressor top surface and discharge temperatures.

To calculate the *COP* of the refrigeration system, cooling capacity is calculated *via* measured temperatures and power input. Figure **6** shows compressor current and power input at 12 VDC voltage supply.

Compressor surface temperature and discharge temperature are illustrated in Figure **7**. This temperatures show us valuable information about the inside temperature level of the compressor.

Total solar radiation in Bornova-Izmir-Turkey, the solar energy powered fridge used, is 5.5, 5.7 and 5.7 kWh m^{-2} for the months May, June and July, respectively. PV tilt angle is 45^{o}. Temperature is the most important effect for the PV energy conversion system since energy conversion efficiency decreases while PV surface temperature increases. PV surface temperature is given in Figure **8**. This temperature level is normal in terms of PV efficiency which is given by the producer. The efficiency of the PV is 14% at this temperature level.

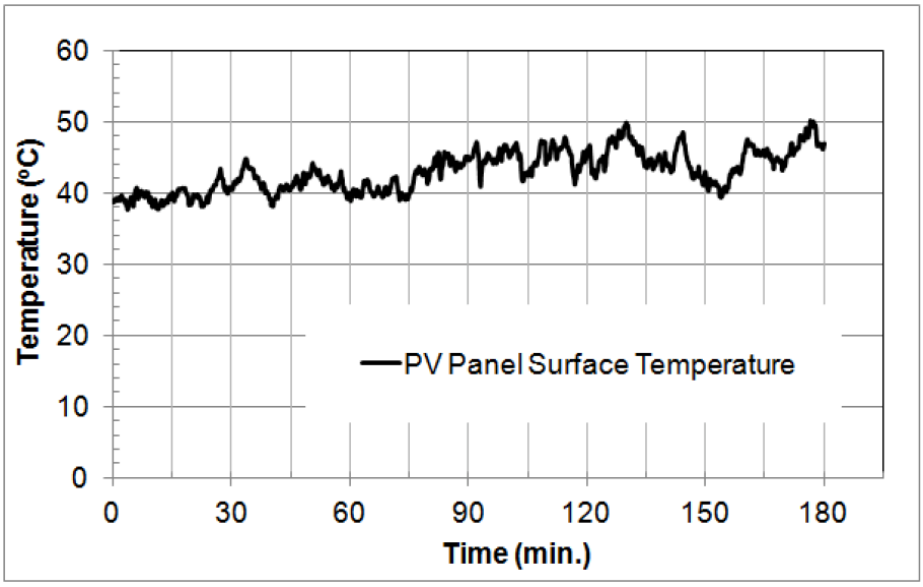

Figure 8: Temperature changes on PV panel surface.

Table 4: Comparison of the Compressors

	Modified DC Compressor	DC Compressor_1 (ACC GD30FDC)	DC Compressor_2 (Danfoss BD35F)
Cooling Capacity (W)	15.0	41.0	43.8
Input Power (W)	49.2	34.0	33.6
COP (-)	0.35	1.21	1.31
COP_{Carnot} (-)	4.2	3.7	3.7
% COP_{Carnot} (-)	8.5	32.5	35.2
η_{comp}	0.2264	0.2739	0.2739
T_{evap} (°C)	-17.3	-15.0	-15.0
T_{cond} (°C)	44.0	55.0	55.0
T_{amb} (°C)	30.4	32.0	32.0

Comparison of the present MDC and the two different BNDCs' catalog data in terms of cooling capacity, input power of the compressor, *COP, COPCar*, percentage of *COPCar* and isentropic efficiency is given in Table **4**.

As it is seen from the table, at the same evaporation temperature MDC's *COP* (0.35) is lower than the others. It consumes high power than others although it has lower cooling capacity (15 W). MDC has bigger *COPCar* because of larger range between the condensing and evaporating temperatures. However, BNDCs use higher percentage of theoretical performance *(*% *COPCar*) which is 32.5% and 35.2% while MDC uses 8.5%. It should also be noted that the BNDCs' isentropic efficiency (%27.39) is higher than the MDC's isentropic efficiency (%22.64).

CONCLUSION

In this study, a reciprocating hermetic AC compressor's stator wires are modified to operate it as a DC compressor. Electrical power of the compressor is 1/15 hp at 12 VDC input voltage and its rotational speed is 2000 rpm. According to brushless DC motor design procedure stator copper wire diameter, total wire length for per phase and number of turns of coils are calculated as 0.3 mm, 5 m and 34 respectively. MDC is powered by solar energy and tested experimentally with respect to cooling capacity, *COP, COPCar*, percentage of *COPCar* and effectiveness of the evaporator.

As a result of the experimental study, it is observed that the MDC has smaller COP compared to the

BNDCs (in Table **4**). This is probably because of large amount of power input in MDC. Large power input may be related with inappropriate electrical motor stator modification. This inappropriate electrical motor operation might also cause high amount of discharge and high surface temperature in compressors. In MDC the electrical motor caused higher current consumption than the BNDCs. This may be related with stator wiring design because total turns of copper wire in the stator affects the current, torque and magnetic field of the motor. High number of turns of wire consumes higher current and provides higher torque in the motor. The effect of the higher torque can also be observed by lower suction pressure than usual level in the compressor.

Furthermore, higher temperature at the compressor affects life of the lubrication oil and the refrigerant, negatively. When the cabinet had higher load the performance of the compressor turned out to be worse (see Table **3**).

As it is resulted from the experiments, the MDC's performance needs to be improved thermodynamically because it uses only 8.5% of theoretical performance (COP_{Car}). Also, its electrical motor should be improved to provide much more cooling than the present with less power consumption.

The used modification procedure should be applied for the AC compressors which have not completed their life cycle yet as well as have electrical motor problem in it. Thus, affordable solar powered mini fridge with DC compressor can be built for the vehicles and/or household usages especially for remote, rural locations used rarely. This is because MDC's performance may not be as well as a BNDC at high utilization level. By this study, it is also shown that a mini fridge can be operated *via* solar energy without any inverter by the current MDC.

NOMENCLATURE

Roman

A	area of cross-section of conductor [mm^2]
B	magnetic field [Weber m^{-2}]
c	capacity [m^3 min^{-1}]
c	specific heat [J kg^{-1} $^oC^{-1}$]
d	cylinder bore radius [m]
I	stator current [Amp]
K	motor constant [-]
l	stator length [m]
L	piston stroke [m]
Lm	mean length of each turn of coil [m]
m	mass flow rate [kg s^{-1}]
N	motor and crankshaft rotational speed [rpm]
N	number of turns [-]
Nc	number of cylinder [-]
P	pressure [bar]
Pm	motor output power [W]
q	heat transfer amount for unit mass [J kg^{-1}]
qcooling	total cooling capacity [W]
R	coil resistance [ohm]
r	solar radiation [W m^{-2}]
S	solar radiation [W m^{-2}]
UA	total heat transfer coefficient [W m^{-2} $^oC^{-1}$]
V	stator voltage [Volt]
T	temperature [˚C]
Td	developed torque [Nm]
W	Power input [W]
w	Radian speed [rad s^{-1}]

Greek

Δ	Variation[–]
ε	Effectiveness [-]
π	Magnetic flux [Weber]
pi	Number (~3.14159) [-]
ρ	Resistivity of conductor [mm m-2]
η	Isentropic efficiency [-]

Subscripts

amb	Ambient
C	Cold side
Cab	Cabinet
Car	Carnot cycle
Ci	Cold side inlet
Co	Cold side outlet
com	Compressor
com_sr	Compressor surface
con	Condenser
cond	Condensing
cpl	Capillary
disc	Discharge
evp	Evaporator
evap	Evaporating
H	Hot side
Hi	Hot side inlet
Ho	Hot side outlet
HX	Heat Exchanger
i	Inlet
max	Maximum
min	Minimum
o	Outlet
pv_srf	Photovoltaic panel surface
R134a	Refrigerant 134a
suc	Suction
inst_tilt	Instant on tilted surface

REFERENCES

[1] Ewert MK, Agrella M, DeMonbrun D, Frahm J, Bergeron DJ and Berchowitz D. Experimental evaluation of a solar PV refrigerator with thermoelectric, stirling and vapour compression heat pumps, *Proceedings of ASES Solar 98 Conference,* Albuquerque, USA, 1998

[2] Kattakayam TA and Srinivasan K. Thermal performance characterization of a photovoltaic driven domestic refrigerator, International Journal of Refrigeration 2000; 23: 190-196. https://doi.org/10.1016/S0140-7007(99)00049-3

[3] Cherif A and Dhouib A. Dynamic modelling and simulation of a photovoltaic refrigeration plant. Renewable Energy 2002; 26: 143-153. https://doi.org/10.1016/S0960-1481(01)00107-0

[4] Kaplanis S and Papanastasiou N. The study and performance of a modified conventional refrigerator to serve as a PV powered one, Renewable Energy 2006; 31: 771-780. https://doi.org/10.1016/j.renene.2005.04.012

[5] Kim DS and Infante Ferreira CA. Solar refrigeration options: a state-of-the-art review. International Journal of Refrigeration 2008; 31: 3-15. https://doi.org/10.1016/j.ijrefrig.2007.07.011

[6] Modi A, Chaudhuri A, Vijay B and Mathur J. Performance analysis of a solar photovoltaic operated domestic refrigerator. Applied Energy 2009; 86: 2583-2591. https://doi.org/10.1016/j.apenergy.2009.04.037

[7] ACC Direct Current Compressor User Manual, September 2006. Received: November 1; 2011. http://www.the-acc-group.com

[8] Danfoss Direct Current and Multivoltage Compressor Datasheet, November 2009. Received: November 1; 2011. http://www.the-acc-group.com

[9] Ekren O. Fuzzy logic control of a compressor and an electronic expansion valve in a chiller. PhD Thesis, Dokuz Eylul University, Graduate School 2009.

[10] Siemens Technical Education Program- Electrical Motor and Control Courses 2011. Received: December 2; 2011. http://sea.siemens.com/step/default.html

[11] Cathey JJ. Electricmachines-Analysis and Design Applying Matlab, first ed., McGraw-Hill, New York 2001.

[12] Skvarenina TL and DeWitt WE. Electrical Power and Control, second ed., Prentice Hall, OH 2001.

[13] Yedemale P. AN885 Brushless DC (BLDC) Motor Fundamentals, Microchip Technology Inc 2003.

Received on 22-11-2017 Accepted on 25-12-2017 Published on 31-12-2017

DOI: http://dx.doi.org/10.15377/2409-5826.2017.04.4